Neurotoxicology 94 (2023) 223–234

Contents lists available at ScienceDirect

Neurotoxicology

journal homepage: www.elsevier.com/locate/neuro

Lutein-loaded nanoparticles reverse oxidative stress, apoptosis, and autism spectrum disorder-like behaviors induced by prenatal valproic acid exposure in female rats

Cristini Escobar Viana [a,b], Vandreza Cardoso Bortolotto [a,b], Stífani Machado Araujo [a,b], Mustafa Munir Mustafa Dahleh [a], Franciéle Romero Machado [a,b], Adson de Souza Pereira [b], Byanca Pereira Moreira de Oliveira [c], Fernanda Vitória Leimann [c,d], Odinei Hess Gonçalves [c,d], Marina Prigol [a,b], Gustavo Petri Guerra [a,b,*]

[a] Laboratório de Avaliações Farmacológicas e Toxicológicas Aplicadas às Moléculas Bioativas – LaftamBio, Universidade Federal do Pampa, Campus Itaqui, 97650–000 Itaqui, RS, Brazil
[b] Programa de Pós-Graduação em Bioquímica, Universidade Federal do Pampa, Campus Uruguaiana, 97508–000 Uruguaiana, RS, Brazil
[c] Programa de Pós-Graduação em Tecnologia de Alimentos, Universidade Tecnológica Federal do Paraná, Campus Campo Mourão, 87301–006 Campo Mourão, PR, Brazil
[d] Centro de Investigação de Montanha (CIMO), ESA, Instituto Politécnico de Bragança, Campus Santa Apolónia, 5300–253 Bragança, Portugal

ARTICLE INFO

Editor: Michael Aschner

Keywords:
Neurodevelopmental disorder
Carotenoid
Social memory
Nanoencapsulation
Sociability
Repetitive behaviors

ABSTRACT

Autism spectrum disorder (ASD) is a neurodevelopmental disorder characterized by deficits in social interaction and repetitive behaviors. In this study, we assessed the effect of lutein-loaded nanoparticles on ASD-like behaviors induced by prenatal valproic acid (VPA) exposure in female offspring rats and the possible involvement of oxidative stress and apoptosis. Pregnant female Wistar rats received a single intraperitoneal injection of VPA (600 mg/kg), on the gestational day 12.5. The VPA-exposed female offspring rats were divided into two subgroups and received either lutein-loaded nanoparticles (5 mg/kg) or saline by oral gavage, for 14 days. The animals were submitted to the three-chamber test and open field to evaluate ASD-like behaviors. The hippocampus was removed for the determination of oxidative stress indicators (ROS; TBARS; SOD and Nrf2) and apoptosis biomarkers (Hsp-70; p38-MAPK; Bax and Bcl-2). The exposure to lutein-loaded nanoparticles reversed sociability deficit, social memory deficit, and anxiety-like and repetitive behaviors induced by VPA, and restored the oxidative stress indicators and apoptosis biomarkers in the hippocampus. This neurochemical effect must be associated with the reversal of ASD-like behaviors. These results provide evidence that lutein-loaded nanoparticles are an alternative treatment for VPA-induced behavioral damage in female rats and suggest the involvement of oxidative stress.

1. Introduction

Autism spectrum disorder (ASD) is a neurodevelopmental disorder diagnosed in early childhood. The main features of ASD include deficits in communication and social interaction, and restricted and repetitive behavior (Modabbernia et al., 2017). In addition, people with ASD develop high levels of anxiety (Kerns et al., 2015). Evidence indicates a higher prevalence of ASD in males (male 4: 1 female) (Crane et al., 2018; Gomes et al., 2015), consequently, most studies on autistic-like behavior have mainly explored the male sex and only a few studies have focused on females or gender differences (Kerr et al., 2016; Liu et al., 2018; Melancia et al., 2018). In this sense, further knowledge about the development of ASD in females is needed, once this subject is still poorly reported, as well as the development of female-specific treatments.

In both patient and animal ASD models, significant neurochemical alterations have been shown, such as an increase in reactive oxygen species, lipid peroxidation, mitochondrial dysfunction, and a decrease in the activity of antioxidant enzymes. These events cause an increase in oxidative stress followed by cell death. Therefore, the association between oxidative stress and apoptosis has emerged as a supposed

* Correspondence to: Universidade Federal do Pampa, Campus Itaqui, Rua Luiz Joaquim de Sá Britto, s/n, Itaqui, Rio Grande do Sul CEP 97650–000, Brazil.
E-mail address: gustavoguerra@unipampa.edu.br (G.P. Guerra).

https://doi.org/10.1016/j.neuro.2022.12.006
Received 30 September 2022; Received in revised form 10 December 2022; Accepted 10 December 2022
Available online 14 December 2022

candidate for the causes of ASD. Additionally, these neurochemical alterations observed in autistic brains often involve the hippocampus. (Bjørklund et al., 2020; Matta et al., 2019).

Considering the increase in the number of children diagnosed with ASD in recent decades and the heterogeneous behavioral symptoms, along with the lack of female-specific treatments and the current treatments, which are limited to behavioral and educational therapies associated with the use of antipsychotics that aim at controlling only some of the symptoms of the disease, the development of new therapeutic options is necessary. In this sense, research on the subject highlights the important role of bioactive compounds, such as carotenoids, which have antioxidant and anti-apoptotic properties (Pereira et al., 2021), considering that oxidative stress and apoptosis contribute to the development of ASD. Interestingly, plasma from patients with ASD has lower levels of carotenoids, when compared to normal children (Krajcovicova-Kudlackova et al., 2009).

Lutein, a fat-soluble xanthophyll carotenoid, is a possible multitarget candidate to prevent/mitigate the symptoms of ASD. Lutein is the main carotenoid found in babies' brains, accounting for more than half of the total concentration of cerebral carotenoids, and it plays an important role in neurodevelopment during the early stages of life (Fitzpatrick and Dhawan, 2014; Vishwanathan et al., 2014). Considering its ability to cross the blood-brain barrier and its preferential uptake when compared to other carotenoids, lutein, the second most prevalent carotenoid in human serum, shows a positive correlation between serum and brain concentrations (Vishwanathan et al., 2014).

Although lutein exhibits biological activities and high therapeutic potential, its use is limited by its low water solubility (Syamila et al., 2019). In fact, there are no studies on the protection promoted by lutein against ASD, even in lutein's raw form (non-encapsulated), which may be related to its low bioavailability. However, studies have shown that lutein nanoparticles have greater bioavailability than free lutein (Arunkumar et al., 2013; Bhat et al., 2020).

Therefore, the present study investigated whether lutein-loaded nanoparticles reverse VPA-induced social deficit, repetitive behavior, and anxiety in female offspring rats, as well as possible mechanisms of action, involving oxidative stress and apoptosis.

2. Materials and methods

2.1. Chemicals

Poloxamer 407 (P407, 12,000.00 g mol^{-1}, Sigma-Aldrich), Tween 80 (Dinâmica), ethanol (Vetec), and lutein (kindly gifted by Kemin S.A) were used in the preparation of lutein-loaded nanoparticles. Valproic acid (VPA) was obtained from Acros Organics (Acros Organics, NJ, USA). Lutein-loaded nanoparticles and VPA were dissolved in a saline solution (0.9% NaCl). All the other reagents used were of analytical grade.

2.2. Nanoparticles production and characterization

Nanoparticles were produced according to the method described by Silva et al. (2017) with minor modifications. Poloxamer 407 and Tween 80 were added to ethanol (120 mL in all experiments) and stirred for 5 min. Then, lutein was added and mixed for 5 min under gentle stirring. The solution was sonicated (Fisher Scientific, 120 W, 1/8′ probe) for 3 min in a pulse regime (30 s on and 10 s off) on an ice bath. Afterward, ethanol was evaporated through air circulation at 40 °C for 24 h and the resulting powder was stored at − 10 °C, protected from light. Table 1 presents the formulation used in the experiments.

The thermal properties of the nanoparticles were analyzed through Differential Scanning Calorimetry (DSC, Perkin Elmer 4000), where samples were heated in aluminum pans (0–300 °C at 20 °C.min^{-1}) under nitrogen flow (50 mL.min^{-1}). Fourier Transform Infrared spectra (FTIR; Frontier Perkin Elmer) was performed in potassium bromide (Sigma-Aldrich, spectroscopic standard) pellets, with a resolution of 2 cm^{-1} from 4500 to 400 cm^{-1} with 32 cumulative scans. Transmission electron microscopy (TEM; JEOL model JEM-1011, 100 kV) was performed to observe the nanoparticles' morphology in parlodium-covered copper grids (300 mesh). The size of the nanoparticles was determined by image analysis after measuring at least 250 particles. In the DSC and FTIR analyses, a mixture of Poloxamer 407 and lutein was obtained by manually mixing these components at the same proportion found in the nanoparticles with the objective of studying the interaction between them.

Table 1
Formulation used in the lutein-loaded nanoparticles production.

	NP1	NP2	NP3	NP4
Lutein concentration (g.g $^{-1}_{P407}$)	0.050	0.067	0.100	0.133
P407 (g)*	1.000	0.750	0.500	0.750
Lutein (g)	0.050	0.050	0.050	0.100
Tween 80 (g)* *	0.010	0.007	0.005	0.006

* Poloxamer 407. * *Concentration of 0.01 g.g P407–1.

2.3. Animals

Male and female Wistar rats (90–120 days old) were used to compose the parental couples. Twenty-eight female offspring were used for the in vivo and ex vivo assays. All the animals were housed in plastic acrylic cages and kept at constant room temperature (21 ± 1 °C) with free access to water and food under a 12:12 h light:dark cycle (lights on at 07:00 h). The behavioral tests were conducted during the light phase of the cycle (from 9:00 a.m. to 5:00 p.m.). All the experiments reported in this study were conducted according to the National and International legislation [guidelines of the Brazilian Council of Animal Experimentation (CONCEA), of the U.S. Public Health Service's Policy on Humane Care and Use of Laboratory Animals (PHS Policy) and the National Institutes of Health guide for the care and use of Laboratory animals (NIH Publications No. 8023, revised 1978) with the approval of the Ethics Committee for Animal Research of the Universidade Federal do Pampa (CEUA protocol nº 041/2018).

2.4. VPA-induced rat model of ASD

Rodents that were prenatally exposed to VPA, on the gestational day 12.5, displayed ASD-like behaviors such as social interaction deficits and anxiety, phenotypes characteristics of the human condition (Kataoka et al., 2013; Schneider et al., 2008; Schneider and Przewłocki, 2005). To obtain offspring with ASD-like behaviors, the methodology described by Singla et al. (2021), including minor modifications, was applied. Male and female rats mated overnight, and in the morning, the presence of spermatozoa in the vaginal smear was confirmed, considering that day zero of gestation (GD 0). On GD 12.5, the females were divided into two groups and received a single intraperitoneal (ip) injection of either VPA (600 mg/kg) or saline (1 mL/kg). The offspring were weaned on the post-natal day 21 (PND 21) and only the female offspring were the subjects of this study. All offspring exposed to VPA during gestation developed the character of a "twist" in the tail (Fig. 1B).

2.5. Lutein-loaded nanoparticles treatment

To investigate whether lutein-loaded nanoparticles reverse VPA-induced social deficit, repetitive behavior, and anxiety in female offspring rats, as well as the possible mechanisms of action involved, on PND 21, the VPA-exposed female offspring were randomly divided into two subgroups and received either lutein-loaded nanoparticles (5 mg/kg) or saline (1 mL/kg) by oral gavage, once a day, for 14 days (PND 21–34). Twenty-four hours after the last injection, the animals were submitted to the three-chamber and open field tests. After the behavioral

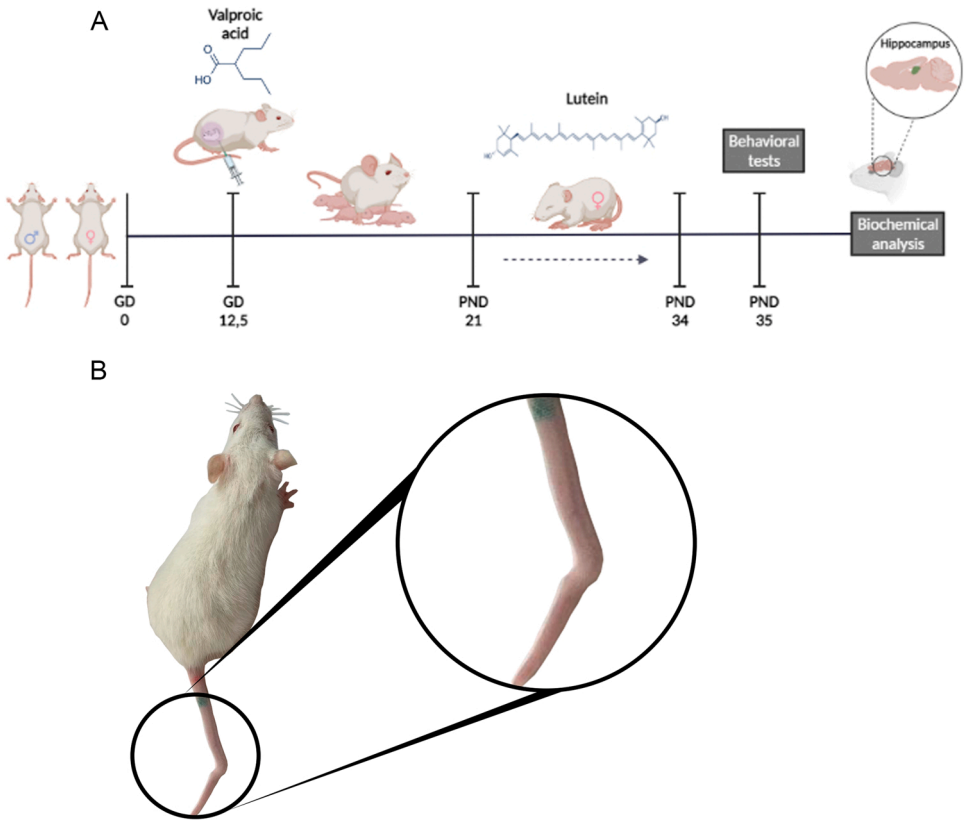

Fig. 1. A) Schematic representation of the experimental design for administration of lutein, for 14 days, in female offspring rats' exposure to VPA. B) Representative photo of crooked tail phenotype prenatal VPA-exposed female offspring.

tests, the hippocampus was removed for the determination of oxidative stress indicators (reactive oxygen species, ROS; thiobarbituric acid reactive substances, TBARS; superoxide dismutase, SOD and nuclear factor E2-related factor 2, Nrf2) and apoptosis biomarkers (Heat shock protein 70, Hsp-70; p38 mitogen-activated protein kinases, p38 MAPK; Bcl-2-associated X protein, Bax and B-cell lymphoma-2, Bcl-2). The dose and administration time were selected based on a previous study that showed lutein-loaded nanoparticles administration (5 mg/kg) does not affect memory (do Prado Silva et al., 2017). The treatment schedule is depicted in Fig. 1A.

2.6. *In vivo assays*

2.6.1. *Three-chamber test*

The three-chamber test was conducted to assess social memory, through social novelty preference, and sociability, as previously described (Castro et al., 2017; Matsuo et al., 2020). The apparatus consisted of a wooden box (60 ×40×30 cm) internally divided into three equal chambers with openings that allow the animals to freely explore the compartments. The test consisted of three sessions: habituation, sociability, and social novelty preference. In the habituation session, the animals were placed into the center chamber and allowed to explore all three chambers for 5 min. In the sociability session, a small plastic cage was placed in both side chambers and a rat that had no previous contact with the subjects (stranger 1) was placed in one of the cages. In the social novelty preference, stranger 1 remained in its cage (now called familiar rat) and another rat with no previous contact with the subjects (stranger 2) was placed in the cage that had been empty during the sociability session. In each session (sociability and social novelty), the subject-animals were placed into the center chamber and allowed to explore all three chambers for 10 min. The time spent exploring each chamber and interacting with each cage was recorded. The sociability index was then calculated, considering the difference of time spent exploring stranger 1 and the empty cage divided by the sum of time spent exploring stranger 1 and the empty cage and used as a sociability parameter (T stranger 1 - T empty cage / T stranger 1 + T empty cage). Analogously, the social novelty index was calculated (T stranger 2 - T familiar rat /T stranger 2 + T familiar rat).

2.6.2. *Open field test*

The open field, a test classically used to assess anxiety-like behavior in rodents, was performed as previously described by (Olexová et al., 2016). Immediately after the three-chamber test, the animals were placed in the corner of the open field apparatus (48 × 48 × 40 cm) facing the wall. During the 10-min open field session, the distance traveled, the time spent in the center, and the time of immobility were recorded. In addition, repetitive behaviors were assessed by monitoring the number of self-grooming.

2.7. *Ex vivo assays*

2.7.1. *Oxidative stress indicators*

Immediately after the open field test, the rats were decapitated, and the hippocampus was removed, weighed, and homogenized in a Tris–HCl (50 mM, pH 7.4) buffer. The resulting homogenate was then centrifuged at 10,000 g for 10 min at 4 °C and the supernatant fraction (S1) was used for the determination of oxidative stress indicators. The protein content was colorimetrically measured using the Bradford method (Bradford, 1976), and BSA (1 mg/mL) was used as the standard.

To estimate levels of reactive oxygen species (ROS) production in the hippocampus, S1 was diluted (1:10) in 50 mM Tris-HCl (pH 7.4) and incubated with 10 μL of 2′,7′-dichlorofluorescein diacetate (DCF-DA; 1 mM) at room temperature for 30 min. The quantification of the DCF-DA oxidation assay was monitored as a general index of oxidative stress

according to the protocol proposed by Loetchutinat et al. (2005). The fluorescence emission resulting from DCF-DA oxidation was monitored and the reading was performed in excitation at 485 nm and 530 nm emission in the spectrophotometer using an EnsPireR multimode microplate reader (Perkin Elmer, USA). The rate of DCF formation was calculated as a percentage of fluorescence treatment relative to the control group.

Lipid peroxidation was estimated by measuring thiobarbituric acid

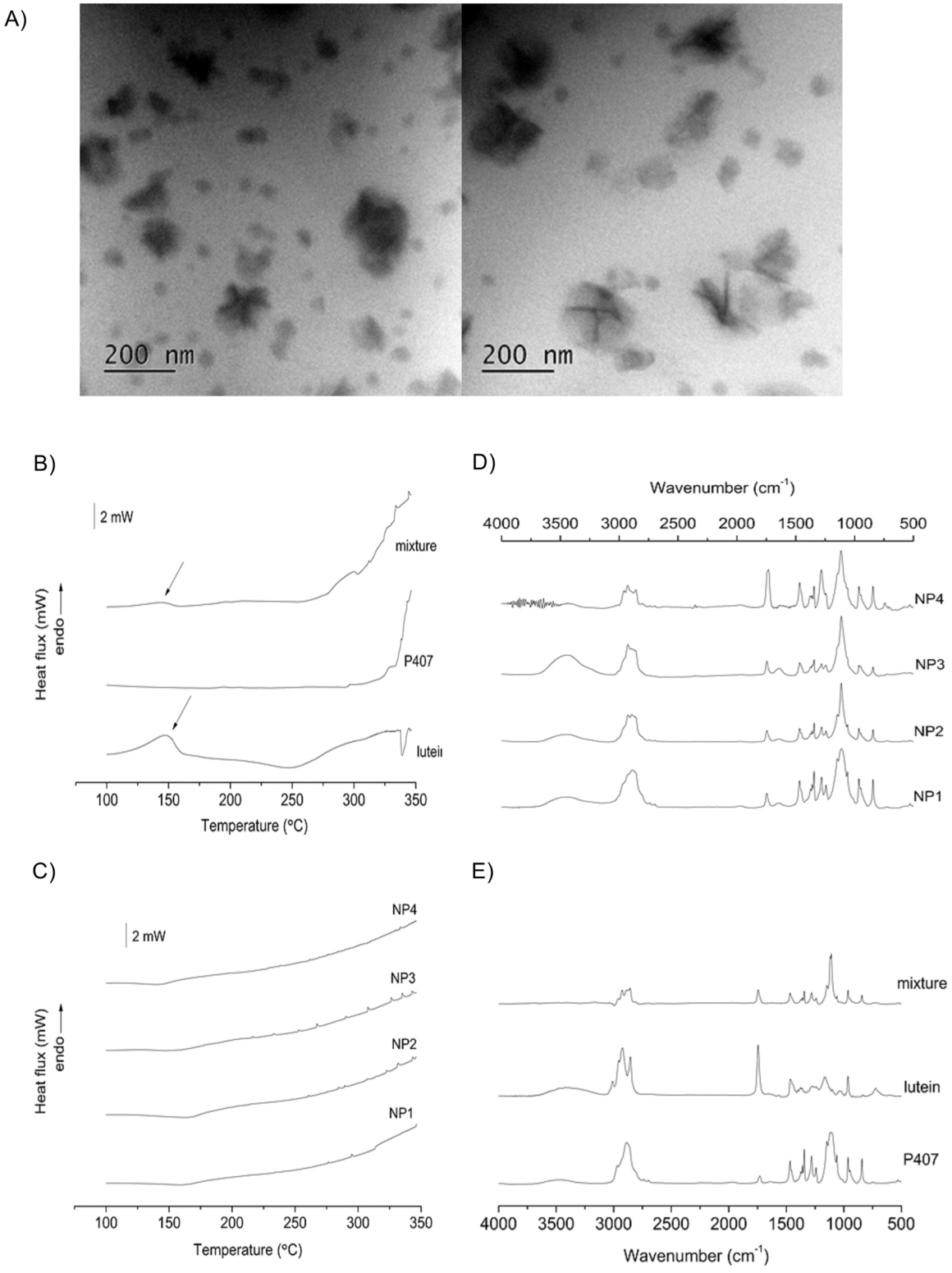

Fig. 2. Physicochemical and morphological characterization of the lutein-loaded nanoparticles A) Images of the lutein-loaded nanoparticles obtained using Transmission Electron Microscopy (formulation NP4–0.133 g.g $^{-1}_{P407}$). B) Differential Scanning Calorimetry curves of lutein, Poloxamer 407, and the mixture of these components. C) Differential Scanning Calorimetry curves of the nanoparticles obtained according to the formulations presented in Table 1. D) Infrared spectra of the nanoparticles obtained according to the formulations presented in Table 1. E) Infrared spectra of lutein, Poloxamer 407, and the mixture of these components.

reactive substance (TBARS) and was expressed in terms of the malondialdehyde (MDA) content, according to the method described by Ohkawa et al. (1979). In this method, MDA, an end product of fatty acid peroxidation, reacts with thiobarbituric acid (TBA) to form a colored complex. The absorbance was measured in the supernatant at 532 nm. The results were calculated as μmol MDA/mg of protein.

2.7.2. Western blot analysis

Western blot analysis was conducted including minor modifications, as previously described (Guerra et al., 2012). Rats were decapitated and the hippocampus was rapidly removed, dissected, and homogenized in 300 μL of ice-cold buffer (10 mM KCl, 2 mM $MgCl_2$,1 mM EDTA, 1 mM NaF, 10 μg/mL aprotinin, 10 mM β-glycerolphosphate, 1 mM PMSF, 1 mM DTT, and 2 mM of sodium orthovanadate in 10 mM HEPES, pH 7.9), incubated on ice for 15 min, and centrifuged at 16,000 g for 45 min at 4 °C. The supernatant was reserved for posterior processing. Protein concentration was determined using the Bradford method (1976). Equivalent amounts of protein (80 μg) were added to 0.2 volumes of concentrated loading buffer (200 mM Tris, 10% glycerol, 2% SDS, 2.75 mM β-mercaptoethanol, and 0.04% bromophenol blue) and boiled for 10 min. Proteins were separated in 12% sodium dodecyl sulfate-polyacrylamide gel electrophoresis (SDS–PAGE) and transferred to polyvinylidene difluoride membranes. Ponceau staining served as a loading control (Romero-Calvo et al., 2010). The membrane was blocked with 1% BSA in 0.05% Tween 20 in Tris-borate saline (TBS-T), then incubated overnight with specific primary antibodies diluted 1: 1000 in TBS-T (anti-Nrf2, anti-SOD, anti-Hsp-70, anti- p38 MAPK, anti-Bax, and anti-Bcl-2 polyclonal antibodies; Santa Cruz Biotechnology, Inc., Santa Cruz, CA, USA). Blots were washed three times with TBS-T followed by incubation with Horseradish peroxidase-conjugated secondary antibody (1: 5000, anti-rabbit IgG; Santa Cruz Biotechnology, Inc.) for 10 min. Protein bands were visualized with 3,3′,5, 5′-Tetramethylbenzidine (TMB; Sigma-Aldrich). Membranes were dried, scanned, and quantified with the Scion Image PC version of the NIH image. The results were normalized by arbitrarily setting the densitometry of the control group as 100%.

2.8. Statistical analysis

The GraphPad Prism 8 software was used for statistical analysis and plotting graphs. Data were checked for normality of distribution using the Shapiro-Wilk test and homogeneity using Bartlett's test. The statistical analyses were performed by a two-way analysis of variance (ANOVA) (lutein-loaded nanoparticles versus VPA), followed by Tukey's post hoc test. Values of $P < 0.05$ were considered statistically significant. All data are expressed as the mean and S.E.M.

3. Results

3.1. Nanoparticles characterization

Thermal and spectroscopic analyses and electron microscopy imaging was carried out to characterize the components used and also the nanoparticles. Fig. 2 (A-E) presents the Transmission Electron Microscopy (TEM) images of the lutein-loaded nanoparticles (formulation NP4–0.133 g.g $^{-1}_{P407}$), the Differential Scanning Calorimetry and the Infrared spectroscopy spectra of lutein, Poloxamer 407, nanoparticles (NP1-NP4) and the lutein-Poloxamer 407 mixture. The melting of Poloxamer407 occurred at 57 °C for all samples (result not shown) while lutein presented a broad endothermic peak at 147 °C. Characteristic groups of lutein can be found at 1370 cm^{-1}, (dimethyl group) 2855 and 2921 cm^{-1} (CH_2 and CH_3 stretching vibrations), and around 3400 cm^{-1} (hydroxyl group). The CH out of the plane bending vibration was present in lutein at 963 and 826 cm^{-1} (do Prado Silva et al., 2017; Grella Miranda et al., 2020; Ranganathan et al., 2016; Silva et al., 2017). Poloxamer 407 exhibited characteristic absorption bands at 2888 cm^{-1} (C-H) and 1110 cm^{-1} (C-O) (Silva de Sá et al., 2019).

3.2. Lutein-loaded nanoparticles reversed VPA-induced social behavior deficit

Fig. 3 (B-G) shows the effect of the exposure to prenatal VPA and oral administration of lutein-loaded nanoparticles (5 mg/kg), for 14 days, on sociability and social novelty preference in the three-chamber test. The statistical analysis (two-way ANOVA) revealed a significant effect of the interaction factor (lutein-loaded nanoparticles versus VPA) on the sociability index [$F_{(1,24)} = 6.65$; $P = 0.0165$]. The post hoc comparisons demonstrated that lutein-loaded nanoparticles reversed the sociability index decrease induced by VPA in the three-chamber test (Fig. 3B).

The statistical analysis (two-way ANOVA) also revealed a significant effect for the interaction factor (lutein-loaded nanoparticles versus VPA) on the time spent in the strange 1 animal chamber [$F_{(1,24)} = 23.77$; $P < 0.0001$] and the empty chamber [$F_{(1,24)} = 15.80$; $P = 0.0006$]. The post hoc comparisons demonstrated that VPA-treated animals spent significantly less time in the strange-1 animal chamber and more time in the empty chamber, compared to the control group. However, animals treated with VPA and lutein-loaded nanoparticles spent significantly more time in the strange-1 animal chamber and less time in the empty chamber compared to the VPA group. The results suggest that lutein-loaded nanoparticles reversed the VPA-induced sociability deficit in the three-chamber test (Fig. 3 C and D).

The statistical analysis (two-way ANOVA) revealed a significant effect of the interaction factor (lutein-loaded nanoparticles versus VPA) on the social novelty preference index [$F_{(1,24)} = 6.94$; $P = 0.0145$]. The post hoc comparisons demonstrated that lutein-loaded nanoparticles reversed the social novelty preference index decrease induced by VPA in the three-chamber test (Fig. 3E). The statistical analysis (two-way ANOVA) also revealed a significant effect for the interaction factor (lutein-loaded nanoparticles versus VPA) on the time spent in the strange 2 animal chamber [$F_{(1,24)} = 27.31$; $P < 0.0001$] and the familiar animal chamber [$F_{(1,24)} = 30.69$; $P < 0.0001$]. The post hoc comparisons demonstrated that VPA-treated animals spent significantly less time in the strange-2 animal chamber and more time in the familiar animal chamber compared to the control group. However, animals treated with VPA and lutein-loaded nanoparticles spent significantly more time in the strange-2 animal chamber and less time in the familiar animal chamber compared to the VPA group. The results suggest that lutein-loaded nanoparticles reversed the VPA-induced social memory deficit in the three-chamber test (Fig. 3 F and G).

3.3. Effect of lutein-loaded nanoparticles on locomotor activity, repetitive behavior, and anxiety-like behavior induced by VPA

Fig. 4 (A-D) shows the effect of the exposure to prenatal VPA and oral administration of lutein-loaded nanoparticles (5 mg/kg), for 14 days, on the locomotor activity, anxiety-like behavior, and repetitive behavior in the open field test. The statistical analysis (two-way ANOVA) showed no significant effect of treatments on the total distance traveled [$F_{(1,24)} = 0.0028$; $P = 0.9582$] (Fig. 4A), suggesting that there was no locomotor damage to the animals. The statistical analysis (two-way ANOVA) also revealed a significant effect for the interaction factor (lutein-loaded nanoparticles versus VPA) on the time spent in the center [$F_{(1,24)} = 9.17$; $P = 0.0058$], time of immobility [$F_{(1,24)} = 8.89$; $P = 0.0065$] and grooming number [$F_{(1,24)} = 6.85$; $P = 0.0151$]. The post hoc comparisons demonstrated that VPA-treated animals spent significantly less time in the center of the apparatus, had more time of immobility, and had a higher grooming number compared to the control group. However, animals treated with VPA and lutein-loaded nanoparticles spent significantly more time in the center of the apparatus, had less time of immobility, and had a smaller grooming number compared to the VPA group. The results suggest that lutein-loaded nanoparticles reversed the anxiety-like behavior, as well as the repetitive behavior

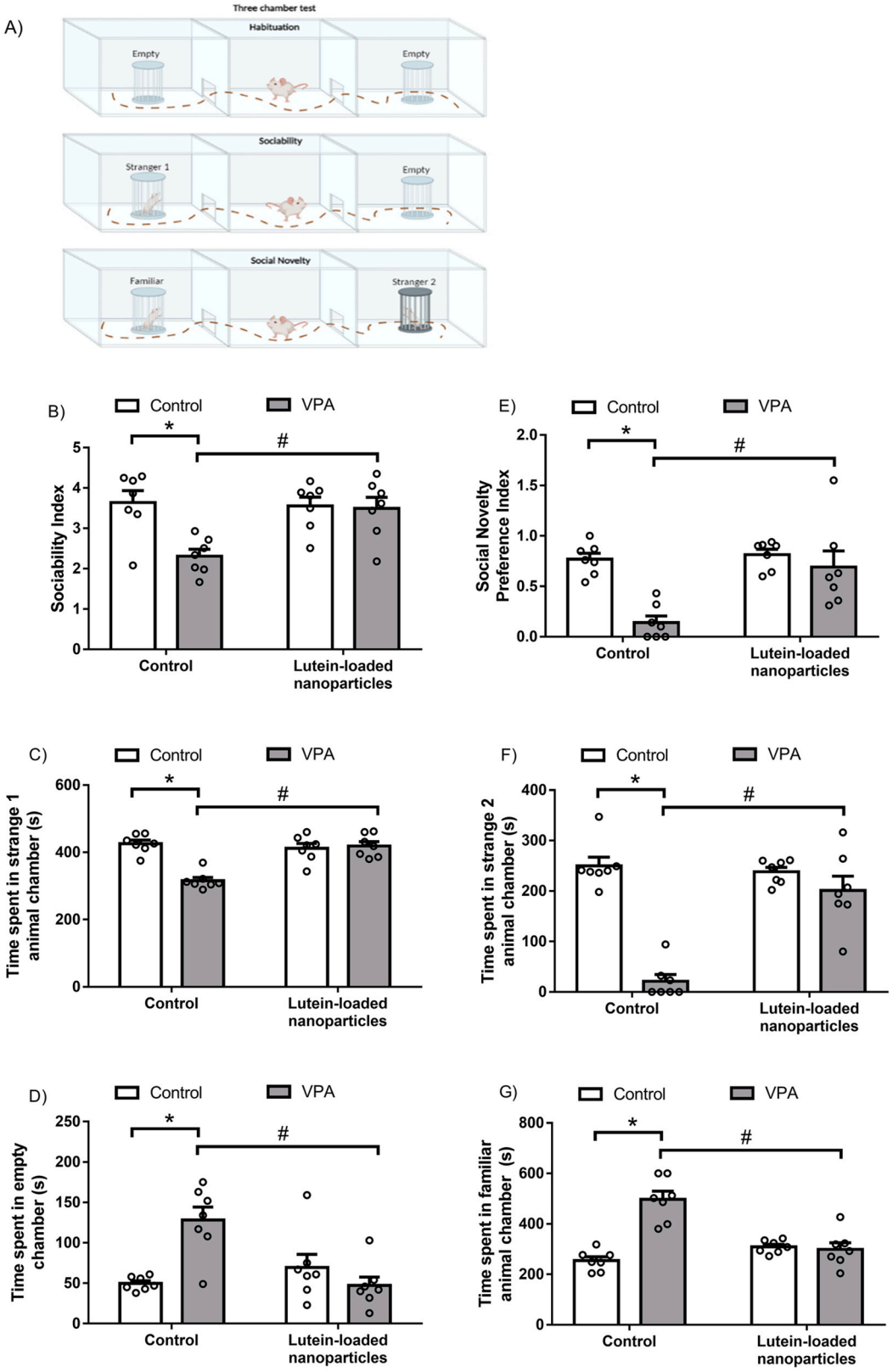

Fig. 3. A) Schematic representation of the three-chamber test used to assess sociability and social novelty preference in rodents. Exposure to prenatal VPA and oral administration of lutein-loaded nanoparticles (5 mg/kg), for 14 days, on the B) Sociability index, C) Time spent in the strange-1 animal chamber, D) Time spent in the empty chamber, E) Social novelty preference index, F) Time spent in the strange-2 animal chamber and G) Time spent in the familiar animal chamber, in the three-chamber test. Data are mean and standard error of the mean (SEM), for n = 7 animals in each group. * Indicates a significant difference ($P < 0.05$) compared to the control group. # Indicates a significant difference ($P < 0.05$) compared to the VPA group.

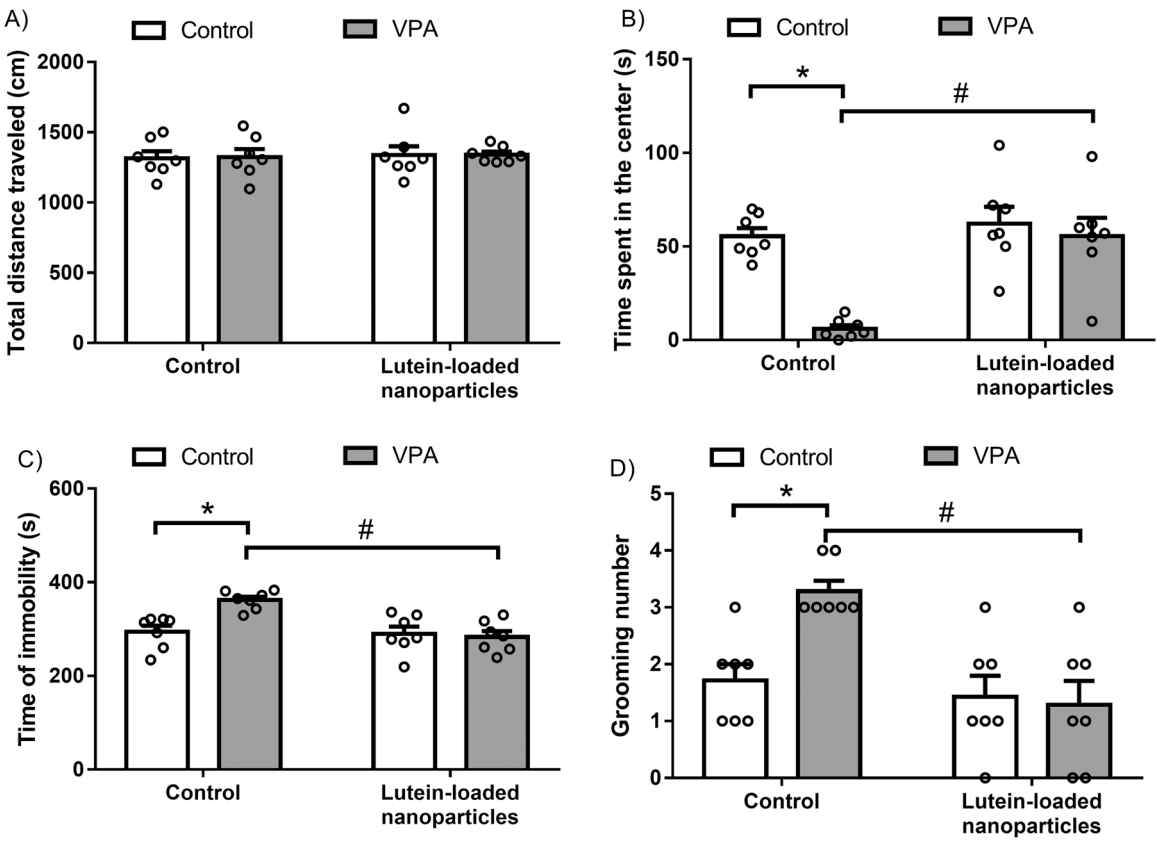

Fig. 4. Exposure to prenatal VPA and oral administration of lutein-loaded nanoparticles (5 mg/kg), for 14 days, on the A) Total distance traveled B) Time spent in the center, C) Time of immobility and D) Grooming number in the open field test. Data are mean and standard error of the mean (SEM), for n = 7 animals in each group. * Indicates a significant difference ($P < 0.05$) compared to the control group. # Indicates a significant difference ($P < 0.05$) compared to the VPA group.

induced by VPA in the open field test (Fig. 4B-D).

3.4. Lutein-loaded nanoparticles reversed VPA-induced oxidative stress indicators alterations

Fig. 5 (A and B) and 6 (A and B) show the effect of the exposure to prenatal VPA and oral administration of lutein-loaded nanoparticles (5 mg/kg), for 14 days, on oxidative stress indicators (ROS and TBARS) and western immunoblotting (Nrf2 and SOD). The statistical analysis (two-way ANOVA) revealed a significant effect for the interaction factor (lutein-loaded nanoparticles versus VPA) on the oxidative stress indicators: ROS [$F_{(1,16)} = 9.19$; $P = 0.0079$] and TBARS [$F_{(1,16)} = 6.35$; $P = 0.0227$] in the hippocampus. The post hoc comparisons demonstrated that lutein-loaded nanoparticles reversed the oxidative stress indicators increase (ROS and TBARS; Fig. 5A and B) induced by VPA in the hippocampus. The statistical analysis (two-way ANOVA) also revealed a significant effect for the interaction factor (lutein-loaded nanoparticles versus VPA) on relative intensive intensity: Nrf2 [$F_{(1,12)} = 16.06$; $P = 0.0017$] and SOD [$F_{(1,12)} = 15.09$; $P = 0.0022$] in the hippocampus. The post hoc comparisons demonstrated that lutein-loaded nanoparticles reversed the relative intensive intensity decrease of Nrf2 (Fig. 6 A) and SOD (Fig. 6B) induced by VPA in the hippocampus.

3.5. Lutein-loaded nanoparticles reversed VPA-induced apoptosis biomarkers alterations

Fig. 7 (A-D) shows the effect of the exposure to prenatal VPA and oral administration of lutein-loaded nanoparticles (5 mg/kg), for 14 days, on apoptosis biomarkers (Hsp-70, p38 MAPK, Bax, and Bcl-2). The statistical analysis (two-way ANOVA) revealed a significant effect for the interaction factor (lutein-loaded nanoparticles versus VPA) on apoptosis biomarkers: Hsp-70 [$F_{(1,12)} = 11.80$; $P = 0.0049$], p38 MAPK [$F_{(1,12)} = 9.81$; $P = 0.0086$], Bax [$F_{(1,12)} = 6.57$; $P = 0.0248$] and Bcl-2 [$F_{(1,12)} = 17.08$; $P = 0.0014$] in the hippocampus. The post hoc comparisons demonstrated that lutein-loaded nanoparticles reversed the relative intensive intensity increase of Hsp-70 (Fig. 7 A), p38 MAPK (Fig. 7B), and Bax (Fig. 7 C), as well as the relative intensive intensity decrease of Bcl-2 (Fig. 7D), induced by VPA in the hippocampus.

4. Discussion

ASD is a neurodevelopmental disorder that includes deficits in social interaction, and restricted and repetitive behavior (Modabbernia et al., 2017). Looking for candidates to prevent/mitigate the symptoms of ASD, our study evaluated the effect of lutein-loaded nanoparticles on ASD-like behaviors induced by prenatal VPA exposure in female offspring rats and the possible mechanism involved. Evidence shows that prenatal exposure of rodents to VPA induces ASD behavioral phenotypes, which are similar to patients with ASD (Kuo and Liu, 2018). Furthermore, deficits in social interaction and repetitive behavior, the major symptoms of ASD, have often been associated with anxiety (Ha et al., 2017). Our results showed that prenatal exposure to VPA induced ASD-like behaviors, such as social interaction and social memory deficits (Fig. 3), and repetitive and anxious behavior (Fig. 4) in female rats. These results confirm what was exposed by Tin-Tin Win-Shwe et al. (2018), who found a deficit of sociability and social novelty preference in both male and female exposure to VPA on day 12.5 of gestation, compared to the corresponding control group. Furthermore, increased repetitive behavior and anxiety-like behaviors in the open field test in female rats exposed to VPA have been reported (Ornoy et al., 2019; Sailer et al., 2019). In line with this view, male and female mice treated

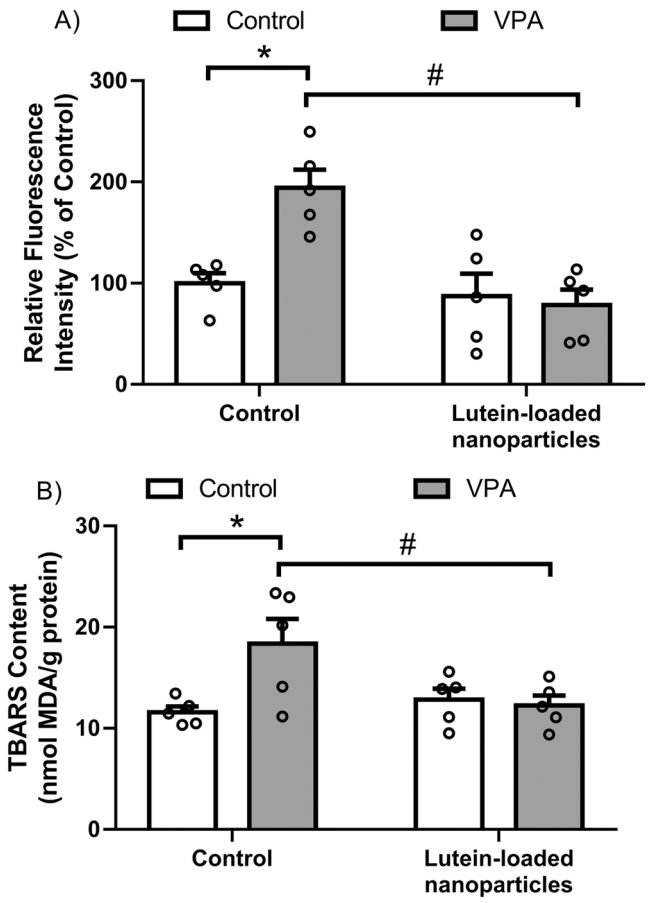

Fig. 5. Exposure to prenatal VPA and oral administration of lutein-loaded nanoparticles (5 mg/kg), for 14 days, on the oxidative stress indicators A) ROS and B) TBARS levels in the hippocampus. Data are mean and standard error of the mean (SEM), for n = 5 animals in each group. * Indicates a significant difference ($P < 0.05$) compared to the control group. # Indicates a significant difference ($P < 0.05$) compared to the VPA group.

with nicotine, in an ASD model, showed an increase in sociability in the three-chamber test and a decrease in repetitive self-grooming behavior in the open field test (Wang et al., 2015). It is also important to note that, although the VPA group spent less time in the strange animal chamber compared to the control, this group spent a long time in the strange animal chamber, corresponding to 53.5% of the total exploration time (considering all chambers). However, our results show that female offspring exposed to VPA had a social behavior deficit, confirmed by the shorter time spent in the strange animal chamber compared to the control group, regardless of the effect intensity.

In the general population, ASD is four times more often in males than in females, therefore, most studies on autistic-like behavior have mainly explored the male sex and few studies have emphasized the female as a subject. However, there are differences not only in the clinical manifestations and behavioral changes but also in the neurochemical alterations of gender-related ASD, in both humans and rodents. Studies have shown that males present ASD-like phenotypes, not observed in females. However, our results showed that prenatal exposure to VPA induced ASD-like behaviors, such as social interaction deficit and social memory deficit and repetitive and anxious behavior in female rats, which must be associated with neurochemical alterations. Therefore, gender differences in disorder characteristics might allow for missed or delayed diagnosis in females. Additionally, the aforementioned information shows the importance of developing specific studies with female subjects, allowing us to understand the disorder characteristics related to gender and the need to seek female-specific therapeutic options.

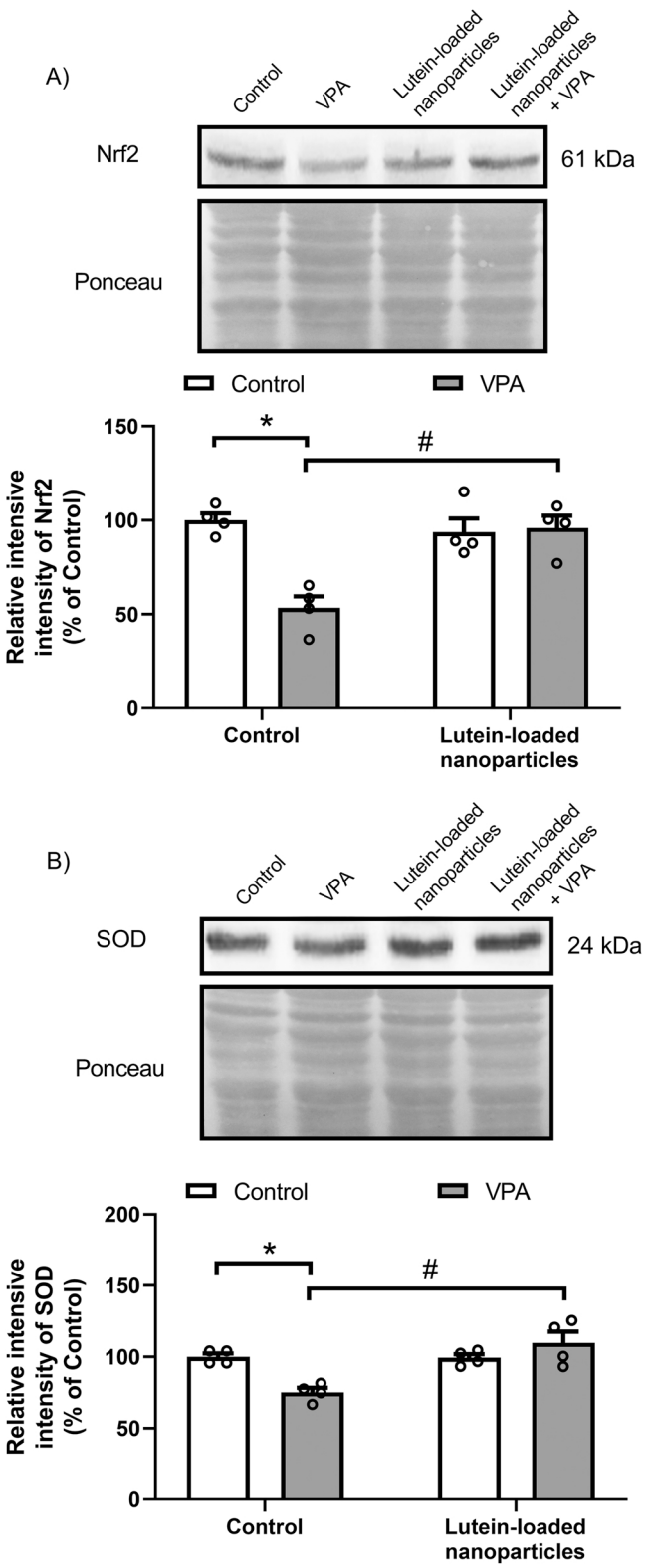

Fig. 6. Exposure to prenatal VPA and oral administration of lutein-loaded nanoparticles (5 mg/kg), for 14 days, on the representative images of Western immunoblotting and densitometry analyses of oxidative stress indicators A) Nrf2 and B) SOD in the hippocampus. The representative Ponceau-stained protein bands demonstrate equal loading. The results were normalized by arbitrarily setting the densitometry of the control group. Data are mean and standard error of the mean (SEM), for n = 4 animals in each group. * Indicates a significant difference ($P < 0.05$) compared to the control group. # Indicates a significant difference ($P < 0.05$) compared to the VPA group.

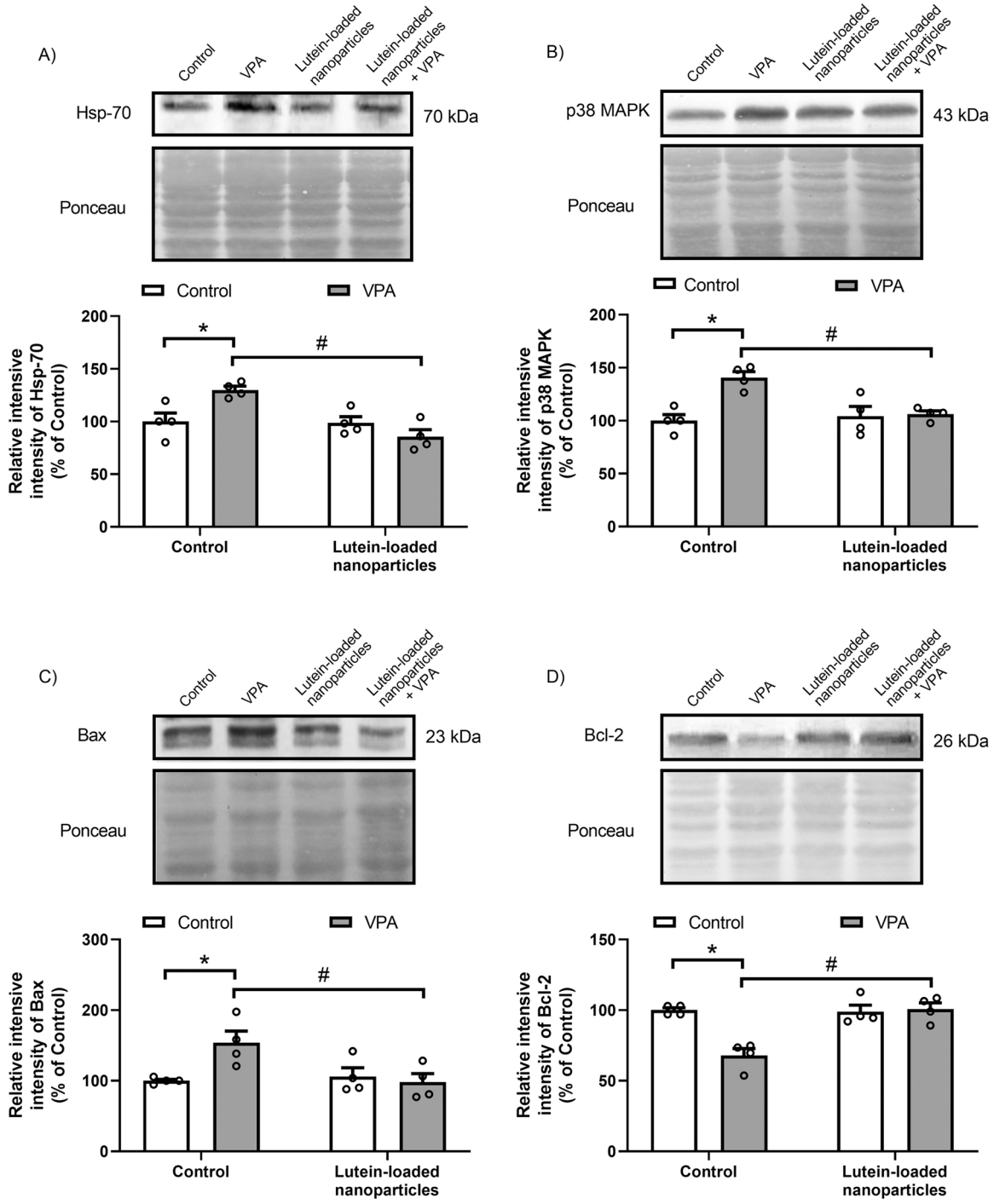

Fig. 7. Exposure to prenatal VPA and oral administration of lutein-loaded nanoparticles (5 mg/kg), for 14 days, on the representative images of Western immunoblotting and densitometry analyses of apoptosis biomarkers A) Hsp-70, B) p38 MAPK, C) Bax and D) Bcl-2 in the hippocampus. The representative Ponceau-stained protein bands demonstrate equal loading. The results were normalized by arbitrarily setting the densitometry of the control group. Data are mean and standard error of the mean (SEM), for n = 4 animals in each group. * Indicates a significant difference ($P < 0.05$) compared to the control group. # Indicates a significant difference ($P < 0.05$) compared to the VPA group.

The great finding of our study is that lutein-loaded nanoparticles reversed the behavioral damage induced by VPA. The neuroprotective effect of lutein has been described for various neurological disorders in different models and species including Huntington's disease (Binawade and Jagtap, 2013), ethanol-induced damage (Geiss et al., 2019), age-related diseases (Johnson, 2012; Kesse-Guyot et al., 2014) and Parkinson disease (Fernandes et al., 2021). Additionally, astaxanthin improved behavioral disorders in a prenatal VPA-induced mice model of autism (Al-Amin et al., 2015), and beta-carotene improved autistic-like behavior in mice (Avraham et al., 2019). However, the effect of lutein, the main carotenoid found in infants' brains, had not yet been demonstrated on ASD-like behaviors. Thus, lutein-loaded nanoparticles reversed the shorter amount of time spent in the strange animal chamber and enhanced self-grooming, as well as the less time spent in the center, suggesting that lutein-loaded nanoparticles improve the damage to sociability, social memory, repetitive behavior, and anxiety induced by

VPA in female offspring rats.

The aforementioned behavioral deficits are likely associated with low activity of antioxidant enzymes, oxidative stress, and apoptosis, which have been considered major contributing factors to ASD (Manivasagam et al., 2020). Furthermore, the increases in oxidative stress may directly induce cell death (Pangrazzi et al., 2020). Interestingly, VPA-induced oxidative stress occurrence is more pronounced in females than in males, evidenced by the increase of MDA in females only (Ornoy et al., 2019). In our study, we observed that prenatal exposure to VPA induced alterations in the oxidative stress indicators, such as increases in ROS and TBARS levels (Fig. 5), and a decrease of Nrf2 and SOD relative intensive intensity (Fig. 6), as well as changes in the apoptosis biomarkers as Hsp-70, p38 MAPK, Bax and Bcl-2 (Fig. 7) in the hippocampus of female rats. The Nrf2 relative intensive intensity decreased was associated with the decreased antioxidant enzyme SOD relative intensive intensity.

Lutein-loaded nanoparticles restored the damage induced by VPA to the neurochemical parameters assessed. This can be evidenced by the neuroprotective effect of lutein on the increases of ROS and TBARS levels, a decrease of Nrf2 and SOD relative intensive intensity, as well as increases of Hsp-70, p38 MAPK, Bax, and a decrease of Bcl-2 relative intensive intensity induced by VPA. The action of lutein as a multi-target antioxidant and anti-apoptotic bioactive compound can be the answer to the protective effect on ASD. This effect must be associated with the structural characteristics of lutein. The long carbon chain with alternating single and double bonds, which can readily accept electrons from reactive species, makes lutein act as a free radicals scavenger. Additionally, the hydroxyl group attached to each end of the molecule contributes to this property (Ahn and Kim, 2021). In this sense, a recent study has shown that lutein-loaded nanoparticles restore the decreased activity of the antioxidant enzymes SOD and catalase, as well as, the increased TBARS levels induced by rotenone in a model of Parkinson's disease in *Drosophila melanogaster* (Fernandes et al., 2021).

The increased activity of antioxidant enzymes and decreased oxidative stress may exert anti-apoptotic effects. Evidence highlights that lutein prevents the downregulation of Bcl2 expression, an anti-apoptotic protein, and the upregulation of Bax expression, a pro-apoptotic protein. Therefore, the lutein-mediated balance of Bax and Bcl-2 effectively maintains the normal apoptotic properties in neurons (Maghsoudi et al., 2021; Tan et al., 2021). Additionally, p38 MAPK is regarded as an important mediator of apoptosis, and its activation has been suppressed by lutein (Tan et al., 2021). On the other hand, Hsp-70 is responsible for protecting cells against injuries by inhibiting apoptosis. The over-expression of Hsp-70 is closely associated with oxidative stress, being an important mechanism involved in the etiology of autism (Mehta et al., 2021). An increase of Hsp-70 was observed in females exposed to VPA, this likely represents a compensatory mechanism seeking to prevent or, at least, reduce cell death in response to increased oxidative stress. Possibly, the administration of lutein counteracted the oxidative stress induced by VPA and, consequently, restored the relative intensive intensity of Hsp-70 to values close to the control group.

We also highlight that lutein-loaded nanoparticles were characterized. The particles presented an average size of (74 ± 6) nm and round morphology which is a characteristic of amorphous solid dispersions. It is worth pointing out that the mixture of Poloxamer and lutein used in the characterization analyses presented the same lutein concentration of the NP4 formulation, which is the highest concentration tested in this study. The DSC curve for the free lutein presented a broad endothermic peak at 147 °C, which is often attributed to lutein degradation (Miguel et al., 2008; Silva de Sá et al., 2019). This peak was also found in the mixture of Poloxamer and lutein but not in the nanoparticles at any of the studied concentrations. This suggests that lutein was protected from degradation at this temperature by the action of the polymeric matrix of Poloxamer. In the FTIR spectra, the attenuation of the absorption bands of lutein can be seen in comparison to the mixture of lutein and Poloxamer obtained manually. TEM, FTIR, and DSC analyses strongly suggest that Poloxamer and lutein formed a solid dispersion during the sonication step and then the amorphous solution of lutein in Poloxamer was achieved. Lutein nanoparticles were obtained using the same method as Silva et al. (2017). They demonstrated that the water solubility of lutein remarkedly increased due to the transformation into nanoparticles.

5. Conclusion

Our results support that the ability of lutein-loaded nanoparticles to inhibit oxidative stress and, consequently, to avoid apoptosis in the hippocampus of female rats must be associated with the reversal of ASD-like behaviors. The reported results promote greater knowledge about the development of ASD in females, which is still poorly reported. We believe that our study provides important insight into lutein-loaded nanoparticles as promising therapeutic agents, allowing for the identification of effective pharmacological strategies in ASD treatment in females. However, further investigation is needed to explore the mechanisms involved in the neuroprotective effects of lutein-loaded nanoparticles on ASD, as well as the possible effects in males with ASD.

CRediT authorship contribution statement

Cristini Escobar Viana: Conceptualization, Formal analysis, Investigation, Writing – original draft, Visualization. **Vandreza Cardoso Bortolotto**: Formal analysis, Investigation. **Stífani Machado Araujo**: Formal analysis, Investigation. **Mustafa Munir Mustafa Dahleh:** Formal analysis, Investigation. **Franciéle Romero Machado**: Formal analysis, Investigation. **Adson de Souza Pereira**: Formal analysis, Investigation. **Byanca Pereira Moreira de Oliveira**: Validation, Investigation. **Fernanda Vitória Leimann:** Resources, Writing – review & editing. **Odinei Hess Gonçalves:** Resources, Writing – review & editing, Visualization. **Marina Prigol:** Conceptualization, Resources, Writing – review & editing. **Gustavo Petri Guerra**: Conceptualization, Formal analysis, Resources, Writing – original draft, Supervision, Project administration.

Declaration of Competing Interest

The authors declare that they have no known competing financial interests or personal relationships that could have appeared to influence the work reported in this paper.

Data Availability

Data will be made available on request.

Acknowledgments

This study was supported by Conselho Nacional de Desenvolvimento Científico e Tecnológico – CNPq (421769/2018–1). Vandreza Cardoso Bortolotto; Stífani Machado Araujo; Franciele Romero Machado; Adson Pereira; Mustafá Dahleh; are the recipient of a FAPERGS or CAPES fellowship. This study was financed in part by the Coordenaç ão de Aperfeiçoamento de Pessoal de N í vel Superior (CAPES) – Finance Code 001. All of the experiments comply with the current laws of Brazil.

References

Ahn, Y.J., Kim, H., 2021. Lutein as a modulator of oxidative stress-mediated inflammatory diseases. Antioxidants 10, 1448. https://doi.org/10.3390/ANTIOX10091448.

Arunkumar, R., Prashanth, K.V.H., Baskaran, V., 2013. Promising interaction between nanoencapsulated lutein with low molecular weight chitosan: characterization and bioavailability of lutein in vitro and in vivo. Food Chem. 141, 327–337. https://doi.org/10.1016/J.FOODCHEM.2013.02.108.

Bhat, I., Yathisha, U.G., Karunasagar, I., Mamatha, B.S., 2020. Nutraceutical approach to enhance lutein bioavailability via nanodelivery systems. Nutr. Rev. 78, 709–724. https://doi.org/10.1093/NUTRIT/NUZ096.

Binawade, Y., Jagtap, A., 2013. Neuroprotective Effect of Lutein Against 3-Nitropropionic Acid–Induced Huntington's Disease–Like Symptoms: Possible Behavioral, Biochemical, and Cellular Alterations, 16, 934–943. https://doi.org/10.1089/JMF.2012.2698.

Bjørklund, G., Meguid, N.A., El-Bana, M.A., Tinkov, A.A., Saad, K., Dadar, M., Hemimi, M., Skalny, A. v, Hosnedlová, B., Kizek, R., Osredkar, J., Urbina, M.A., Fabjan, T., El, A.A., 2020. Oxidative stress in autism spectrum disorder. Joanna Kałużna-Czaplińska 57, 2314–2332. https://doi.org/10.1007/s12035-019-01742-2.

Bradford, M.M., 1976. A rapid and sensitive method for the quantitation of microgram quantities of protein utilizing the principle of protein-dye binding. Anal. Biochem. 72, 248–254. https://doi.org/10.1016/0003-2697(76)90527-3.

Castro, K., Baronio, D., Perry, I.S., Riesgo, R., dos, S., Gottfried, C., 2017. The effect of ketogenic diet in an animal model of autism induced by prenatal exposure to valproic acid. Nutr. Neurosci. 20, 343–350. https://doi.org/10.1080/1028415X.2015.1133029.

Crane, Batty, L., Richard, Adeyinka, Hanna, Goddard, Henry, L., Hill, L.A., E.L, 2018. Autism diagnosis in the united kingdom: perspectives of autistic adults, parents and professionals. J. Autism Dev. Disord. 48, 3761–3772. https://doi.org/10.1007/s10803-018-3639-1.

Fernandes, E.J., Poetini, M.R., Barrientos, M.S., Bortolotto, V.C., Araujo, S.M., Santos Musachio, E.A., de Carvalho, A.S., Leimann, F.V., Gonçalves, O.H., Ramborger, B.P., Roehrs, R., Prigol, M., Guerra, G.P., 2021. Exposure to lutein-loaded nanoparticles attenuates Parkinson's model-induced damage in Drosophila melanogaster: Restoration of dopaminergic and cholinergic system and oxidative stress indicators. Chem. -Biol. Interact. 340, 109431 https://doi.org/10.1016/J.CBI.2021.109431.

Fitzpatrick, E., Dhawan, A., 2014. Noninvasive biomarkers in non-alcoholic fatty liver disease: Current status and a glimpse of the future. World J. Gastroenterol.: WJG 20, 10863. https://doi.org/10.3748/WJG.V20.I31.10851.

Geiss, J.M.T., Sagae, S.C., Paz, E.D.R., de Freitas, M.L., Souto, N.S., Furian, A.F., Oliveira, M.S., Guerra, G.P., 2019. Oral administration of lutein attenuates ethanol-induced memory deficit in rats by restoration of acetylcholinesterase activity. Physiol. Behav. 204, 121–128. https://doi.org/10.1016/J.PHYSBEH.2019.02.020.

Gomes, P.T.M., Lima, L.H.L., Bueno, M.K.G., Araújo, L.A., Souza, N.M., 2015. Autism in Brazil: a systematic review of family challenges and coping strategies. Braz.: a Syst. Rev. Fam. Chall. coping Strateg. J. De. Pediatr. 91, 111–121. https://doi.org/10.1016/j.jped.2014.08.009.

Grella Miranda, C., dos Santos, P.D.F., do Prado Silva, J.T., Vitória Leimann, F., Ferreira Borges, B., Miguel Abreu, R., Porto Ineu, R., Hess Gonçalves, O., 2020. Influence of nanoencapsulated lutein on acetylcholinesterase activity: In vitro determination, kinetic parameters, and in silico docking simulations. Food Chem. 307, 125523 https://doi.org/10.1016/J.FOODCHEM.2019.125523.

Guerra, G.P., Mello, C.F., Bochi, G. v, Pazini, A.M., Rosa, M.M., Ferreira, J., Rubin, M.A., 2012. Spermidine-induced improvement of memory involves a cross-talk between protein kinases C and A. J. Neurochem. 122, 363–373. https://doi.org/10.1111/J.1471-4159.2012.07778.X.

Ha, S., Park, H., Mahmood, U., Ra, J.C., Suh, Y.H., Chang, K.A., 2017. Human adipose-derived stem cells ameliorate repetitive behavior, social deficit and anxiety in a VPA-induced autism mouse model. Behav. brain Res. 317, 479–484. https://doi.org/10.1016/J.BBR.2016.10.004.

Johnson, E.J., 2012. A possible role for lutein and zeaxanthin in cognitive function in the elderly 1-5. Am. J. Clin. Nutr. 96, 1161s–1165s. https://doi.org/10.3945/ajcn.112.034611.

Kataoka, S., Takuma, K., Hara, Y., Maeda, Y., Ago, Y., Matsuda, T., 2013. Autism-like behaviours with transient histone hyperacetylation in mice treated prenatally with valproic acid. Int. J. Neuropsychopharmacol. 16, 91–103. https://doi.org/10.1017/S1461145711001714.

Kerns, C.M., Kendall, P.C., Zickgraf, H., Franklin, M.E., Miller, J., Herrington, J., 2015. Not to be overshadowed or overlooked: functional impairments associated with comorbid anxiety disorders in youth with ASD. Behav. Ther. 46, 29–39. https://doi.org/10.1016/J.BETH.2014.03.005.

Kerr, D.M., Gilmartin, A., Roche, M., 2016. Pharmacological inhibition of fatty acid amide hydrolase attenuates social behavioural deficits in male rats prenatally exposed to valproic acid. Pharmacol. Res. 113, 228–235. https://doi.org/10.1016/J.PHRS.2016.08.033.

Kesse-Guyot, E., Andreeva, V.A., Ducros, V., Jeandel, C., Julia, C., Hercberg, S., Galan, P., 2014. Carotenoid-rich dietary patterns during midlife and subsequent cognitive function. Br. J. Nutr. 111, 915–923. https://doi.org/10.1017/S0007114513003188.

Krajcovicova-Kudlackova, M., Valachovicova, M., Mislanova, C., Hudecova, Z., Sustrova, M., Ostatnikova, D., 2009. Plasma concentrations of selected antioxidants in autistic children and adolescents. Bratisl. Lek. Listy 110, 247–250. https://europepmc.org/article/med/19507654.

Kuo, H.Y., Liu, F.C., 2018. Molecular pathology and pharmacological treatment of autism spectrum disorder-like phenotypes using rodent models. Front. Cell. Neurosci. 12, 422. https://doi.org/10.3389/FNCEL.2018.00422/BIBTEX.

Liu, F., Horton-Sparks, K., Hull, V., Li, R.W., Martínez-Cerdeño, V., 2018. The valproic acid rat model of autism presents with gut bacterial dysbiosis similar to that in human autism. Mol. Autism 9, 1–13. https://doi.org/10.1186/S13229-018-0251-3/FIGURES/6.

Loetchutinat, C., Kothan, S., Dechsupa, S., Meesungnoen, J., Jay-Gerin, J.P., Mankhetkorn, S., 2005. Spectrofluorometric determination of intracellular levels of reactive oxygen species in drug-sensitive and drug-resistant cancer cells using the 2′,7′-dichlorofluorescein diacetate assay. Radiat. Phys. Chem. 72, 323–331. https://doi.org/10.1016/J.RADPHYSCHEM.2004.06.011.

Maghsoudi, S., Taghavi Shahraki, B., Rabiee, N., Fatahi, Y., Bagherzadeh, M., Dinarvand, R., Ahmadi, S., Rabiee, M., Tahriri, M., Hamblin, M.R., Tayebi, L., Webster, T.J., 2021. The colorful world of carotenoids: A profound insight on therapeutics and recent trends in nano delivery systems, 62. Taylor & Francis, pp. 3658–3697. https://doi.org/10.1080/10408398.2020.1867958.

Manivasagam, T., Arunadevi, S., Essa, M.M., SaravanaBabu, C., Borah, A., Thenmozhi, A. J., Qoronfleh, M.W., 2020. Role of oxidative stress and antioxidants in autism. Adv. Neurobiol. 24, 193–206. https://doi.org/10.1007/978-3-030-30402-7_7.

Matsuo, K., Yabuki, Y., Fukunaga, K., 2020. 5-aminolevulinic acid inhibits oxidative stress and ameliorates autistic-like behaviors in prenatal valproic acid-exposed rats. Neuropharmacology 168, 107975. https://doi.org/10.1016/J.NEUROPHARM.2020.107975.

Matta, S.M., Hill-Yardin, E.L., Crack, P.J., 2019. The influence of neuroinflammation in Autism Spectrum Disorder. Brain, Behav., Immun. 79, 75–90. https://doi.org/10.1016/J.BBI.2019.04.037.

Mehta, R., Bhandari, R., Kuhad, A., 2021. Effects of catechin on a rodent model of autism spectrum disorder: implications for the role of nitric oxide in neuroinflammatory pathway. Psychopharmacol. (Berl.) 238, 3249–3271. https://doi.org/10.1007/S00213-021-05941-5/TABLES/6.

Melancia, F., Schiavi, S., Servadio, M., Cartocci, V., Campolongo, P., Palmery, M., Pallottini, V., Trezza, V., 2018. Sex-specific autistic endophenotypes induced by prenatal exposure to valproic acid involve anandamide signalling. Br. J. Pharmacol. 175, 3699–3712. https://doi.org/10.1111/BPH.14435.

Miguel, F., Martín, A., Mattea, F., Cocero, M.J., 2008. Precipitation of lutein and co-precipitation of lutein and poly-lactic acid with the supercritical anti-solvent process. Chem. Eng. Process. 47, 1594–1602. https://doi.org/10.1016/j.cep.2007.07.008.

Modabbernia, A., Velthorst, E., Reichenberg, A., 2017. Environmental risk factors for autism: an evidence-based review of systematic reviews and meta-analyses. Mol. Autism 8, 1–16. https://doi.org/10.1186/s13229-017-0121-4.

Ohkawa, H., Ohishi, N., Yagi, K., 1979. Assay for lipid peroxides in animal tissues by thiobarbituric acid reaction. Anal. Biochem. 95, 351–358. https://doi.org/10.1016/0003-2697(79)90738-3.

Olexová, L., Štefánik, P., Kršková, L., 2016. Increased anxiety-like behaviour and altered GABAergic system in the amygdala and cerebellum of VPA rats — an animal model of autism. Neurosci. Lett. 629, 9–14. https://doi.org/10.1016/J.NEULET.2016.06.035.

Ornoy, A., Weinstein-Fudim, L., Tfilin, M., Ergaz, Z., Yanai, J., Szyf, M., Turgeman, G., 2019. S-adenosyl methionine prevents ASD like behaviors triggered by early postnatal valproic acid exposure in very young mice. Neurotoxicol. Teratol. 71, 64–74. https://doi.org/10.1016/J.NTT.2018.01.005.

Pangrazzi, L., Balasco, L., Bozzi, Y., 2020. Oxidative stress and immune system dysfunction in autism spectrum disorders. Int. J. Mol. Sci. 21, 3293. https://doi.org/10.3390/IJMS21093293.

Pereira, A.G., Otero, P., Echave, J., Carreira-Casais, A., Chamorro, F., Collazo, N., Jaboui, A., Lourenço-Lopes, C., Simal-Gandara, J., Prieto, M.A., 2021. Xanthophylls from the sea: algae as source of bioactive carotenoids. Mar. Drugs 19, 188. https://doi.org/10.3390/MD19040188.

Ranganathan, A., Hindupur, R., Vallikannan, B., 2016. Biocompatible lutein-polymer-lipid nanocapsules: acute and subacute toxicity and bioavailability in mice. Mater. Sci. Eng.: C. 69, 1318–1327. https://doi.org/10.1016/J.MSEC.2016.08.029.

Sailer, L., Duclot, F., Wang, Z., Kabbaj, M., 2019. Consequences of prenatal exposure to valproic acid in the socially monogamous prairie voles. Sci. Rep. 9, 1–14. https://doi.org/10.1038/s41598-019-39014-7.

Schneider, T., Przewłocki, R., 2005. Behavioral alterations in rats prenatally exposed to valproic acid: animal model of autism. Neuropsychopharmacology 30, 80–89. https://doi.org/10.1038/sj.npp.1300518.

Schneider, T., Roman, A., Basta-Kaim, A., Kubera, M., Budziszewska, B., Schneider, K., Przewłocki, R., 2008. Gender-specific behavioral and immunological alterations in an animal model of autism induced by prenatal exposure to valproic acid. Psychoneuroendocrinology 33, 728–740. https://doi.org/10.1016/j.psyneuen.2008.02.011.

Silva, J.T., do, P., Silva, A.C., da, Geiss, J.M.T., de Araújo, P.H.H., Becker, D., Bracht, L., Leimann, F.V., Bona, E., Guerra, G.P., Gonçalves, O.H., 2017. Analytical validation of an ultraviolet–visible procedure for determining lutein concentration and application to lutein-loaded nanoparticles. Food Chem. 230, 336–342. https://doi.org/10.1016/J.FOODCHEM.2017.03.059.

Silva de Sá, I., Peron, A.P., Leimann, F.V., Bressan, G.N., Krum, B.N., Fachinetto, R., Pinela, J., Calhelha, R.C., Barreiro, M.F., Ferreira, I.C.F.R., Gonçalves, O.H., Ineu, R. P., 2019. In vitro and in vivo evaluation of enzymatic and antioxidant activity, cytotoxicity and genotoxicity of curcumin-loaded solid dispersions. Food Chem. Toxicol. 125, 29–37. https://doi.org/10.1016/J.FCT.2018.12.037.

Singla, R., Mishra, A., Joshi, R., Kumar, R., Sarma, P., Sharma, A.R., Kaur, G., Bhatia, A., Medhi, B., 2021. Inhibition of the ERK1/2 phosphorylation by dextromethorphan protects against core autistic symptoms in VPA induced autistic rats: in silico and in vivo drug repurposition study. ACS Chem. Neurosci. 12, 1749–1767. https://doi.org/10.1021/ACSCHEMNEURO.0C00672.

Syamila, M., Gedi, M.A., Briars, R., Ayed, C., Gray, D.A., 2019. Effect of temperature, oxygen and light on the degradation of β-carotene, lutein and α-tocopherol in spray-dried spinach juice powder during storage. Food Chem. 284, 188–197. https://doi.org/10.1016/J.FOODCHEM.2019.01.055.

Tan, X., Liang, Z., Li, Y., Zhi, Y., Yi, L., Bai, S., Forest, K.H., Nichols, R.A., Dong, Y., Li, Q. X., 2021. Isoorientin, a GSK-3β inhibitor, rescues synaptic dysfunction, spatial memory deficits and attenuates pathological progression in APP/PS1 model mice. Behav. Brain Res. 398, 112968 https://doi.org/10.1016/J.BBR.2020.112968.

Vishwanathan, R., Kuchan, M.J., Sen, S., Johnson, E.J., 2014. Lutein and preterm infants with decreased concentrations of brain carotenoids. J. Pediatr. Gastroenterol. Nutr. 59, 659–665. https://doi.org/10.1097/MPG.0000000000000389.

Wang, L., Almeida, L.E.F., Spornick, N.A., Kenyon, N., Kamimura, S., Khaibullina, A., Nouraie, M., Quezado, Z.M.N., 2015. Modulation of social deficits and repetitive behaviors in a mouse model of autism: the role of the nicotinic cholinergic system. Psychopharmacol. (Berl.) 232, 4303–4316. https://doi.org/10.1007/S00213-015-4058-Z/FIGURES/7.

Win-Shwe, T.T., Nway, N.C., Imai, M., Lwin, T.T., Mar, O., Watanabe, H., 2018. Social behavior, neuroimmune markers and glutamic acid decarboxylase levels in a rat model of valproic acid-induced autism. J. Toxicol. Sci. 43, 631–643. https://doi.org/10.2131/JTS.43.631.